Optimal Motion Planning for Localization of Avalanche Victims by Multiple UAVs

Camilla Tabasso, *Graduate Student Member, IEEE*, Nicola Mimmo, Venanzio Cichella, *Member, IEEE*, and Lorenzo Marconi

***Abstract*—This letter proposes a method for localization of avalanche victims by multiple UAVs. The method consists of three main parts. First, assuming that the UAVs and the victim are equipped with ARTVA receivers and a transmitter, respectively, we introduce a mathematical model of the receiver, which is used to estimate the position of the victim. Second, we derive a closed-form expression indicating the performance of this estimator. In particular, we show that the victim's observability index is captured by the persistency of excitation of a function of the UAVs trajectories. Third, we design and implement a motion planning algorithm that uses the estimation and the estimator's performance function for the (near) real-time generation of trajectories that guarantee feasible, safe, and time-efficient localization of avalanche victims.**

***Index Terms*—Optimal motion planning, Bernstein polynomials, ARTVA sensors, observability-based planning.**

I. Introduction

SEARCH and Rescue (S&R) robots have become increasingly attractive for their ability to support humans in different disaster areas [1]–[4]. Several studies have focused on high mountain scenarios where Unmanned Aerial Vehicles (UAVs) are asked to localize avalanche victims [5], [6]. To achieve this goal, the UAVs are equipped with a device called *ARTVA*[1] *receiver*, which senses and processes the electromagnetic field emitted by the *ARTVA transmitter* (carried by the avalanche victim). The main idea, which was originally presented in [5], [6], is to develop ARTVA-driven control and estimation laws for the identification of the transmitter's location. This letter in [7], [8] shows that a single UAV tracking a sufficiently excited reference trajectory (composed by sums of sin functions in the 3D space) is able to estimate the location of the victim. It was demonstrated that the estimation performance depends on the trajectory excitation level, which is proportional to the amplitude and frequency of the sin functions. In practice, to track this aggressive reference, the UAV must perform acrobatic maneuvers that rapidly reduce the battery life and thus the support that the UAV can provide to the S&R mission.

In this letter we explore the use of multiple UAVs, by means of a cooperative trajectory generation algorithm, to design less demanding but still excited trajectories. The objective of the algorithm is to generate trajectories for multiple vehicles that maximize the reliability of the target position's estimation, while minimizing the vehicles' control effort, and satisfying a set of constraints. These constraints include feasibility and inter-vehicle safety constraints to guarantee safe unfolding of the mission. Thus, the trajectory generation algorithm must be able to handle possibly complex optimal control problems.

The problem of planning and control for target estimation has received a great deal of attention in the research community, see [9]–[12] and citations therein. For example, an optimal control theoretical framework is employed in [9], [12], where the trajectory generation problem is formulated as an optimal control problem aimed at maximizing an *estimation performance index*. The problem is then solved by means of closed-loop controllers based on online gradient descent [9] or MPC [12]. However, when dealing with cooperative S&R missions involving multiple UAVs in a real-world environment, optimal control problems that arise from this application are very complex. The cost function and constraints involved can be highly nonlinear, non-smooth, and non-convex, and closed-loop solutions cannot be formulated. Therefore, solutions to these problems must be sought through numerical methods [13]. Numerical methods such as direct methods are based on approximating optimal control problems into nonlinear programming problems (NLPs) using some discretization scheme [13]–[16]. Then, these NLPs can be solved using off-the-shelf optimization solvers (e.g., MATLAB, SNOPT, etc.). A wide range of direct methods that use different discretization schemes have been developed, including Euler [17],

Manuscript received September 14, 2020; revised November 26, 2020; accepted December 19, 2020. Date of publication January 5, 2021; date of current version March 26, 2021. This work was supported in part by the European Project "Aerlal RoBotic technologies for professiOnal seaRch aNd rescuE" (AirBorne), Call: H2020, ICT-25-2016/17, under Grant 780960, and in part by the Air Force Research Laboratory ARCTOS CRDINAL Project under Grant FA8650-16-C-2642. Recommended by Senior Editor L. Menini. *(Corresponding author: Camilla Tabasso.)*

Camilla Tabasso and Venanzio Cichella are with the Department of Mechanical Engineering, University of Iowa, Iowa City, IA 52240 USA (e-mail: camilla-tabasso@uiowa.edu; venanzio-cichella@uiowa.edu).

Nicola Mimmo and Lorenzo Marconi are with the Department of Electrical and Information Engineering "Guglielmo Marconi," University of Bologna, 40126 Bologna, Italy (e-mail: nicola.mimmo2@unibo.it; lorenzo.marconi@unibo.it).

Digital Object Identifier 10.1109/LCSYS.2021.3049314

[1]ARTVA stands for the Italian "Apparecchio di Ricerca dei Travolti in VAlanga"

2475-1456 © 2021 IEEE. Personal use is permitted, but republication/redistribution requires IEEE permission.
See https://www.ieee.org/publications/rights/index.html for more information.

Authorized licensed use limited to: Universita degli Studi di Roma La Sapienza. Downloaded on July 13,2023 at 11:03:11 UTC from IEEE Xplore. Restrictions apply.

Runge-Kutta [18], [19], Pseudospectral [20], as well as methods based on Bernstein approximants [21], [22].

In the context of the existing literature on autonomous systems planning and control for target estimation, this work differs from other approaches in a fundamental way. Rather than dealing with simplified problems and designing closed-loop controllers, we formulate the multi-vehicle target estimation problem as a general nonlinear optimal planning problem and find an approximate solution using a direct method. We employ the direct method based on Bernstein approximants that was initially proposed in [23]. Bernstein approximants possess nice geometric and numerical properties, and provide algorithms that are particularly useful for the computation and enforcement of feasibility and inter-vehicle safety distance constraints. Furthermore, using the properties highlighted in [21], it is possible to generate trajectories for multi-vehicle missions in a (near) real-time fashion. Here we exploit these properties and algorithms to address the problem of target position's estimation. For more in depth discussion on the benefits of Bernstein polynomial-based approaches as compared to other direct methods for trajectory generation, the reader is referred to [23]–[26]. This approach allows us to consider multi-objective scenarios where the vehicles must efficiently estimate the position of a target while minimizing mission execution time, actuation effort, and guarantee inter-vehicle safety for the whole duration of the mission. To ensure robustness to estimator faults and guarantee convergence to the victim, we propose an event-triggered approach to re-plan trajectories for the whole mission duration (rather than for a shorter receding horizon) using up-to-date estimates.

This letter is organized as follows. This section ends with the description of the notation. Section II represents a brief recap of the ARTVA model and introduces the estimation algorithm. Section III and IV state the optimization problem and presents its solution with numerical results described in Section V. Finally, in Section VI we discuss the results and draw the conclusions.

A. Notations

Given n matrices $x_i \in \mathbb{R}^{n_i \times m}$ with $i = 1, \dots, n$, and $n, n_i, m \in \mathbb{N}^+$, we define the column operator $\mathtt{col}(\cdot) : \mathbb{R}^{n_1 \times m} \times \cdots \times \mathbb{R}^{n_n \times m} \to \mathbb{R}^{(\sum_{i=1}^n n_i) \times m}$ as

$$\mathtt{col}(x_1, \dots, x_n) = \begin{bmatrix} x_1 \\ \vdots \\ x_n \end{bmatrix}.$$

Finally, we define a non decreasing function $s : \mathbb{R} \to \mathbb{N}$ that associates to the current time t, the number of ARTVA samples from 0 to t, i.e., $s(t)$. The i-th sample time is denoted by τ_i with $\tau_0 \geq 0$ and $\tau_{s(t)} \leq t$.

II. The ARTVA Transmitter Localization

We consider a single ARTVA transmitter and $n \in \mathbb{N}$ receivers, each of them rigidly attached to an UAV. Let $p_k(\tau_i) \in \mathbb{R}^3$ denote the inertial position of the k-th UAV at the sample time τ_i, with $k, i \in \mathbb{N}$ and $k = 1, \dots, n$. Moreover, let the position of the transmitter be denoted by $p_t \in \mathbb{R}^3$. As described in [7], the intensity of the ARTVA signal can be approximated by an output modelled as $y : \mathbb{R}^3 \times \mathbb{R} \to \mathbb{R}$,

$$y(p_k, \tau_i) = \Phi^\top(p_k)\mathrm{x}(p_t) + \delta(p_k - p_t) + v_t(p_k - p_t, \tau_i), \quad (1)$$

where $p_k = \mathtt{col}(x_k, y_k, z_k)$,

$$\Phi(p_k) = \mathtt{col}(x_k^2,\ 2x_k y_k,\ 2x_k z_k,\ y_k^2,\ 2y_k z_k,\ z_k^2,\ -2x_k,\ -2y_k,\ -2z_k,\ 1) \quad (2)$$

is a known signal, and

$$\mathrm{x}(p_t) = \mathtt{col}(\overline{m}_{11}, \overline{m}_{12}, \overline{m}_{13}, \overline{m}_{22}, \overline{m}_{23}, \overline{m}_{33}, \overline{p}_t, \varrho) \quad (3)$$

is the vector of the unknown constants. The terms $\overline{m}_{ij} \in \mathbb{R}$, with $i, j = 1, 2, 3$, represent the entries of $\overline{M} := [\overline{m}_{ij}]$, with $\overline{M} = \overline{M}^\top \in \mathbb{R}^{3\times 3}$, $\overline{p}_t := \overline{M}p_t$, and $\varrho := p_t^\top \overline{M} p_t$. Moreover, $\delta(\cdot) : \mathbb{R}^3 \to \mathbb{R}$ represents the model mismatch introduced by the approximation and $v(\cdot, \cdot) : \mathbb{R}^3 \times \mathbb{R} \to \mathbb{R}$ is the contribution to y of the measurement noise.

Remark 1: Both $\delta(p_k - p_t)$ and $v(p_k - p_t, t)$ are class-$\mathcal{K}_\infty$ functions of $\|p_k - p_t\|$ meaning that they go to zero for $\|p_k - p_t\| \to 0$. Moreover, a detailed analysis of $v(p_k - p_t, t)$ reveals that it is proportional to $\|p_k - p_t\|^5$ thus implying that $v(p_k - p_t, t) = o(\Phi^\top(p_k)\mathrm{x}(p_t))$ for $\|p_k - p_t\| \to 0$. In simple words, this means that the output is more informative if the UAV becomes closer to the transmitter. Finally, it can be shown that the term $\delta(p_k - p_t)$ satisfies $|\delta(p_k - p_t) - \Phi^\top(p_k)\mathrm{x}(p_t)|/|\Phi^\top(p_k)\mathrm{x}(p_t)| < 0.06$ for each $p_k \in \mathbb{R}^3$.

A. Estimation of the Transmitter Location

In the context of the S&R missions under consideration, the number of vehicles available is usually small (from 1 to 10 typically [5]) and the search space is typically smaller than a few thousands square meters. Thus, it is reasonable to assume the presence of a communication network with static topology on which we can implement a centralized estimation algorithm. A similar architecture has been successfully tested in [27].

To estimate the constant vector p_t, we consider the position of the k-th vehicle, $p_k(\tau_i)$, to be known, and collect all the available data in the network in the following centralized model

$$Y(\tau_i) = H^\top(\tau_i)\mathrm{x}(p_t) + \Delta(\tau_i) + V(\tau_i), \quad (4)$$

with

$$\begin{aligned} Y(\tau_i) &= \mathtt{col}(y(p_1(\tau_i), \tau_i), \dots, y(p_n(\tau_i), \tau_i)), \\ H^\top(\tau_i) &= \mathtt{col}(\Phi^\top(p_1(\tau_i)), \dots, \Phi^\top(p_n(\tau_i))), \\ \Delta(\tau_i) &= \mathtt{col}(\delta(p_1(\tau_i) - p_t), \dots, \delta(p_n\tau_i) - p_t)), \\ V(\tau_i) &= \mathtt{col}(v(p_1(\tau_i) - p_t, \tau_i), \dots, v(p_n(\tau_i) - p_t, \tau_i)). \end{aligned}$$

The model in (4) can be used to estimate the constant vector x, exploiting the knowledge of the affine term $H(\tau_i)$, by means of the following Recursive Least Squares (RLS) [28]

$$\hat{\mathrm{x}}(\tau_{i+1}) = \hat{\mathrm{x}}(\tau_i) + S^{-1}(\tau_i)H(\tau_i)\Big(Y(\tau_i) - H^\top(\tau_i)\hat{\mathrm{x}}(\tau_i)\Big), \quad (5a)$$

$$S(\tau_{i+1}) = \beta S(\tau_i) + H(\tau_i)H^\top(\tau_i), \quad (5b)$$

Authorized licensed use limited to: Universita degli Studi di Roma La Sapienza. Downloaded on July 13,2023 at 11:03:11 UTC from IEEE Xplore. Restrictions apply.

in which $\beta \in (0, 1)$ and $S(\tau_0) = S_0 = S_0^\top \succ 0$ with $S_0 \in \mathbb{R}^{3\times 3}$. Then, we estimate the position of the transmitter as

$$\hat{p}_t(\tau_i) = \mathrm{x}^{-1}(\hat{\mathrm{x}}(\tau_i)), \tag{5c}$$

in which $\mathrm{x}^{-1}(\cdot) : \mathbb{R}^{10} \to \mathbb{R}^3$ is well posed, as demonstrated in [7].

Remark 2: We employ RLS methods based on the assumption that an accurate positioning system is available (ideal GPS). On the other hand, Total Least Square (TLS) methods can be adopted to consider noisy data affected by disturbance and errors.

Any linear regression algorithm such as the RLS [28], the Kalman filter [29] or, in case of noisy $H(\tau_i)$, the Total Least Squares and the Errors in Variables methods [30], work on the same common assumption, i.e., that $S(\tau_i) \succ 0$ for any $i \in \mathbb{N}$. This assumption is translated into the positive definiteness of the *determinability* Gramian (see [9]) which is fulfilled if $H(\tau_i)$ is sufficiently exciting. More in detail, since

$$\begin{aligned} S(\tau_i) &= \beta^i S_0 + \sum_{j=0}^{i-1} \beta^{i-1-j} H(\tau_j) H^\top(\tau_j) \\ &\succeq \beta^{i-1} \sum_{j=0}^{i-1} H(\tau_j) H^\top(\tau_j), \end{aligned} \tag{6}$$

$H(\cdot)$ is said to be *Persistently Exciting* (PE) if, given $m \in \mathbb{N}^+$, there exists a positive real $\alpha_0 > 0$ such that $\forall s(t) \geq m$, $\mathcal{O}(s(t), m) \succeq \alpha_0 I$ with

$$\mathcal{O}(s(t), m) := \frac{1}{m} \sum_{i=s(t)-m+1}^{s(t)} H(\tau_i) H^\top(\tau_i). \tag{7}$$

This letter defines as *observability performance index* the minimum singular value of (7), denoted as $\underline{\sigma}(s(t), m)$.

Remark 3: For the case of $n = 1$ (single receiver), it has been shown in [7], [8] that the excitation level is linked to the complexity of the reference trajectories $\tau_i \mapsto p_1(\tau_i)$. Since such complex trajectories are demanding from the point of view of the energy consumption and the difficulty of the trajectory tracking task, in this letter we want to exploit the presence of multiple vehicles to keep the persistent excitation level while reducing the trajectory complexity. As an intuitive support to our approach, Figure 1 shows that the observability performance index $\underline{\sigma}(s(t), m)$ increases whether the trajectories become more complex or the number of UAVs increases. On one hand, the rank of $H(\tau_i)H^\top(\tau_i)$ increases with the number of UAVs. On the other hand, more exciting trajectories for the UAVs lead to higher values of $\underline{\sigma}(s(t), m)$. For instance, given a constant number of 5 UAVs, $\underline{\sigma}(s(t), m)$ changes depending on whether the UAV is hovering, or tracking a circular or a ∞-shaped trajectory. On the other hand, for a given trajectory, the number of UAVs increases the value of $\underline{\sigma}(s(t), m)$.

III. Problem Formulation

In this letter, we focus on the generation of desired trajectories of n ARTVA receivers for estimation of the location of a single ARTVA transmitter. We consider vehicles whose

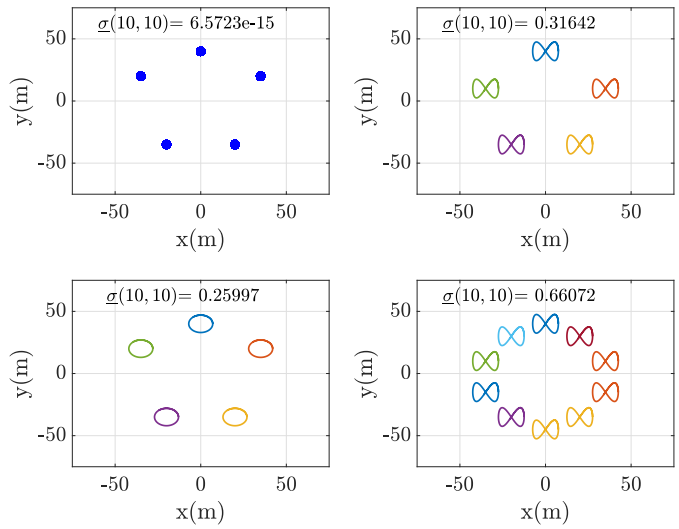

Fig. 1. Effect of the shape of the trajectory (left) and the number of vehicles (right) on $\underline{\sigma}(s(t), m)$.

dynamics are stabilized by on-board controllers able to provide trajectory tracking capabilities. This allows us to focus on the design of desired trajectories, namely $p_{d,k}(t)$ with $k = 1, \ldots, n$, with bounded first and second derivatives, trackable by the vehicles. We refer to [31]–[34], where it is shown that given such trajectories, one can design a nonlinear controller that enables the UAV to converge to it. For the sake of simplicity, we assume that the vehicles are able to perfectly track their desired trajectories, i.e., $p_{d,k}(t) = p_k(t)$, for all $t \geq 0$. With this in mind, the aim is to find desired trajectories $p^*_{d,k}(t)$, and minimal final mission time t^*_f that minimize actuation effort and maximize the observability performance index. The trajectory generation problem can be formulated as follows.

Problem 1: For given initial time t_0 and estimated transmitter position computed at time t_0, $\hat{p}_t(\tau_{s(t_0)})$ (see Equation (5)),

$$\begin{aligned} \min_{p_{d,k}(t),\, t_f} \quad & w_1(t_f - t_0) + w_2 \sum_{k=1}^{n} \int_{t_0}^{t_f} ||\ddot{p}_{d,k}(\tau)||^2 \, d\tau \\ & - w_3 \underline{\sigma}(s(t_f), s(t_f) - s(t_0)), \end{aligned} \tag{8}$$

with $w_1,\ w_2,\ w_3 > 0$, subject to

$$p_{d,k}(t_0) = p_{k,t_0}, \dot{p}_{d,k}(t_0) = \dot{p}_{k,t_0}, \tag{9a}$$

$$||p_{d,k}(t_f) - \hat{p}_t(\tau_{s(t_0)})|| \leq \delta_t, \tag{9b}$$

$$||p_{d,k}(t) - p_{d,j}(t)|| \geq d_{safe} \quad t \in [t_0, t_f], \tag{9c}$$

$$||\dot{p}_{d,k}(t)|| \leq v_{k,max}, \quad t \in [t_0, t_f], \tag{9d}$$

for all $k, j = 1, \ldots, n$, $k \neq j$ and with δ_t, d_{safe}, $v_{k,max} > 0$.

Remark 4: The boundary conditions in Equation (9a) ensure continuity of the reference and its first derivative at time t_0. The end point constraint in Equation (9b) guarantees arrival of the receiver at a δ_t-neighborhood of the estimated position of the transmitter. The design parameter δ_t must be selected large enough in order to allow satisfaction of the inter-vehicle safety constraint, represented by (9c), at the end point. Inequality (9d) ensures that the reference trajectories can be tracked by the receivers. The parameters d_{safe} and $v_{k,max}$ are

Authorized licensed use limited to: Universita degli Studi di Roma La Sapienza. Downloaded on July 13,2023 at 11:03:11 UTC from IEEE Xplore. Restrictions apply.

given positive constants denoting the minimum safe distance between two vehicles and the maximum allowed speed, and depend on the vehicle and the mission at hand.

Remark 5: One of the main challenges when dealing with multi-vehicle missions is the need to guarantee safety amongst agents. Despite the fact that inter-vehicle safety can be guaranteed by having the UAVs fly on different search planes, aerodynamics interference could arise from two vehicles flying directly above or below each other. Thus, we include (9c).

IV. Trajectory Generation Using Bernstein Approximants

Due to its complexity, the problem defined in the previous section cannot be solved analytically. In contrast to approaches in the literature that simplify the problem at hand and compute solutions in closed-loop fashion, e.g., [9], [12], here we employ numerical methods to approximate open-loop optimal solutions to Problem 1. In particular, we employ the direct method that uses Bernstein polynomial approximation to transcribe optimal control problems as finite-dimensional optimization problems [21]. The motivation is that Bernstein polynomials offer favorable geometric properties that are particularly useful when dealing with trajectory generation for multi-vehicle missions [23], [24]. Let the desired trajectory to be tracked by the k-th UAV, i.e., $p_{d,k} : [t_0, t_f] \to \mathbb{R}^3$, be approximated by a N-th order Bernstein polynomial

$$p_{d,k}(t) \approx p_{N,k}(t) = \sum_{j=0}^{N} \bar{p}_{j,N}^{[k]} b_{j,N}(t), \quad t \in [t_0, t_f], \tag{10}$$

where $\bar{p}_{0,N}^{[k]}, \ldots, \bar{p}_{N,N}^{[k]} \in \mathbb{R}^3$ are Bernstein polynomial coefficients, and

$$b_{j,N}(t) = \binom{N}{j} \frac{(t-t_0)^j (t_f - t)^{N-j}}{(t_f - t_0)^N}, \quad t \in [t_0, t_f],$$

for $j = 0, \ldots, N$, is the N-th order Bernstein basis, and $\binom{N}{j} = \frac{N!}{j!(N-j)!}$ is the binomial coefficient. The following properties of Bernstein polynomials are used in this letter.

Property 1 (Differentiation and integration): The derivatives of the Bernstein polynomial $p_{N,k}(t)$ can be easily computed as

$$\begin{aligned} \dot{p}_{N,k}(t) &= \sum_{i=0}^{N} \sum_{j=0}^{N} \bar{p}_{j,N}^{[k]} D_{j,i} b_{i,N}(t), \\ \ddot{p}_{N,k}(t) &= \sum_{i=0}^{N} \sum_{j=0}^{N} \bar{p}_{j,N}^{[k]} D_{j,i}^2 b_{i,N}(t), \end{aligned} \tag{11}$$

where $D_{j,k}$ is the (j,k)-th entry of a square differentiation matrix [21]. The integral of $p_{N,k}(t)$ is computed as

$$\int_{t_0}^{t_f} p_{N,k}(t) dt = w \sum_{j=0}^{N} \bar{p}_{j,N}^{[k]}, \quad w = \frac{t_f - t_0}{N+1}. \tag{12}$$

Property 2 (Arithmetic operations): The sum (difference) of two N-th order Bernstein polynomials is an N-th order Bernstein polynomial. The product between two Bernstein polynomials of orders N and M is a Bernstein polynomial of order $N + M$ [26, Ch. 5].

Using Properties 1 and 2, the following functions can be expressed as Bernstein polynomials:

$$\begin{aligned} ||\dot{p}_{N,k}(t)||^2 &= \sum_{j=0}^{2N} \bar{v}_{j,N}^{[k]} b_{j,N}(t), \\ ||p_{N,k}(t) - p_{N,i}(t)||^2 &= \sum_{j=0}^{2N} \bar{d}_{j,N}^{[ki]} b_{j,N}(t). \end{aligned} \tag{13}$$

In the equation above, $\bar{v}_{j,N}^{[k]}$ $\forall j \in \{0, \ldots, 2N\}$, can be obtained from algebraic manipulation of the Bernstein coefficients of $p_{N,k}(t)$. Similarly, $\bar{d}_{j,N}^{[ki]}$ can be obtained from the Bernstein coefficients of $p_{N,k}(t)$ and $p_{N,i}(t)$.

Property 3 (End point values): The initial and final values of a Bernstein polynomial are equal to its first and last Bernstein coefficients, e.g., $p_{N,k}(t_0) = \bar{p}_{0,N}^{[k]}$ and $p_{N,k}(t_f) = \bar{p}_{N,N}^{[k]}$.

Property 4 (Evaluating Bounds and Extrema [25], [35]): There exist computationally efficient algorithms to evaluate upper and lower bounds (or actual extrema) of a Bernstein polynomial by straightforward operations on its Bernstein coefficients. These algorithms are presented in [25], [35] and the open-source implementation is available at [36].

With this setup, let the Bernstein coefficients describing the n UAVs trajectories be $\bar{p}_{j,N} = \texttt{col}(\bar{p}_{j,N}^{[0]}, \ldots, \bar{p}_{j,N}^{[n]}) \in \mathbb{R}^{3n}$, for all $j = 0, \ldots, N$. Then, Problem 1 can be re-stated as follows.

Problem 2: For given time t_0 and estimated transmitter position computed at time t_0, i.e., $\hat{p}_t(\tau_{s(t_0)})$,

$$\begin{aligned} \min_{\bar{p}_{0,N}, \ldots, \bar{p}_{N,N}, t_f} \quad & w_1(t_f - t_0) + w_2 \sum_{k=1}^{n} \int_{t_0}^{t_f} ||\ddot{p}_{N,k}(\tau)||^2 \, d\tau \\ & - w_3 \underline{\sigma}(s(t_f), s(t_f) - s(t_0)), \end{aligned} \tag{14}$$

subject to

$$p_{N,k}(t_0) = p_{k,t_0}, \dot{p}_{N,k}(t_0) = \dot{p}_{k,t_0}, \tag{15a}$$

$$||p_{N,k}(t_f) - \hat{p}_t(\tau_{s(t_0)})|| \leq \delta_t, \tag{15b}$$

$$||p_{N,k}(t) - p_{N,j}(t)||^2 \geq d_{safe}^2, \quad t \in [t_0, t_f], \tag{15c}$$

$$||\dot{p}_{N,k}(t)||^2 \leq v_{k,max}^2, \quad t \in [t_0, t_f], \tag{15d}$$

for all $k, j = 1, \ldots, n$, $k \neq j$, and with w_1, w_2, $w_3 > 0$.

By virtue of Properties 1-4, the above problem results into a nonlinear programming problem, which can be solved using off-the-shelf nonlinear optimization solvers. In particular, the integral in the cost function can be computed by combining Equations (12) and (13). Constraints (15a) and (15b) can be enforced by using Property 3. Finally, inequalities (15c) and (15d) can be imposed using Property 4.

Remark 6: Theoretical results concerning the existence of a feasible solution to Problem 2 can be derived using similar steps as the ones outlined in [24]. Moreover, it can be shown that by increasing the order of approximation N in Equation (10), the solution to Problem 2 converges uniformly to that of Problem 1.

Authorized licensed use limited to: Universita degli Studi di Roma La Sapienza. Downloaded on July 13,2023 at 11:03:11 UTC from IEEE Xplore. Restrictions apply.

A. Event-Triggered Re-Planning

As described in Remark 1, the estimation error is smaller if the ARTVA data are sampled closer to the transmitter location. Thus, since the location of the transmitter is unknown, we steer the UAVs toward the estimated transmitter location, provided by (5). The data collected while steering the formation toward the last estimated location are exploited to refine the estimation. For this reason, we re-plan the fleet trajectory to exploit the most up-to-date estimation. The re-planning framework is described in the remainder of this section.

At time intervals $\bar{t}$, a new estimate of the transmitter's location is calculated taking into account the new data gathered by the UAVs. Then, the following re-planning conditions are evaluated given $\bar{t}$, ϵ, $\rho > 0$.

1) $\|\hat{p}_t(t) - \hat{p}_t(t-\bar{t})\| \leq \rho$
2) $\underline{\sigma}(s(t), m) > \epsilon$

The conditions above ensure that the new estimate is in the neighbourhood of the previous one (condition 1), and the last estimation is reliable (condition 2). If both of them are satisfied, the vehicles continue on their current trajectories, otherwise new trajectories are calculated where $t_0 = t$ and the final mission time t_f is re-evaluated. This re-planning strategy constitutes a loop between the estimation and the motion planning. Future work will address the stability of this loop, following steps similar to the ones introduced in [7].

Remark 7: The use of Bernstein polynomials and their properties at the motion planning level makes the implementation of this framework (near) real-time possible.

V. Numerical Results

In this section, we propose the results of a S&R mission simulated on MATLAB. In this scenario, 5 UAVs equipped with ARTVA receivers, are tasked to estimate the position of the transmitter, and to generate feasible trajectories to reach its location. The trajectories are approximated using 5th order Bernstein polynomials, and are computed using MATLAB `fmincon` to solve the optimization problem presented in Section IV.

For this scenario, the feasibility constraints are set to $v_{k,max} = 5$ m/s, $d_{safe} = 3$ m, and $\delta_t = 5$ m. The evaluation of the re-planning conditions takes place at intervals $\bar{t} = 10s$ and new trajectories are generated if $\|\hat{p}_t(t) - \hat{p}_t(t-\bar{t})\| \leq \rho = 2$ m and $\underline{\sigma}(s(t), s(t)) > \epsilon = 0.7$. These parameters are arbitrarily chosen and can be tuned based on the type of UAVs available. Figure 2 shows the evolution of the mission at four time instances. At $t = 0$ s, the vehicles' trajectories are planned to reach a "pentagon formation" to cover the search area. It can be seen that as time progresses, a better estimate of the transmitter location is calculated. At $t = 40$ s, $\underline{\sigma}(s(t), s(t)) = 0.822$. However, since $\|\hat{p}_t(t) - \hat{p}_t(t-\bar{t})\| = 3.997$ m, a trajectory re-planning is triggered. Conversely, at $t = 50$ s, both criteria for re-planning are satisfied, and therefore the vehicles keep following their trajectories instead of re-planning. Finally, at $t_f = 53.23$ s, the mission is successfully terminated. For this simulation the computational time for each trajectory re-plan is 0.5 s on average (ran on Lenovo ThinkPad with Intel Core i7-8550U, 1.80GHz CPU), which demonstrates the feasibility of near real-time implementation of the proposed algorithm. The computational time can be further reduced by using different software, optimization solvers, and higher computing power.

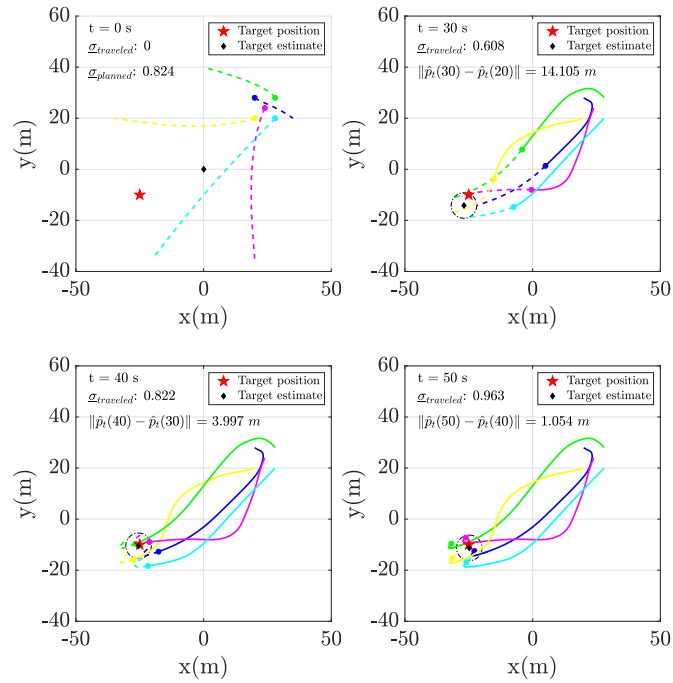

Fig. 2. Execution of the mission at four time instances. The dots show the current position of the vehicles, while the solid lines represent the trajectory already traveled, and the dashed lines represent the portion of the trajectory yet to cover. Finally, the position of the target is shown by the red star, while the estimate of its position is shown by the black diamond.

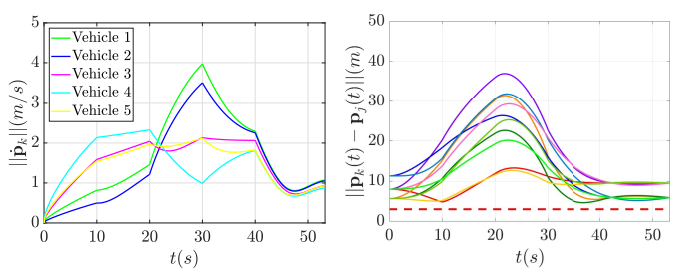

Fig. 3. (Left) Velocity profiles, (right) inter-vehicle distances.

We note that if in this scenario the re-planning strategy was not adopted, the UAVs would move towards their first estimation of the victim's location, which is likely incorrect. This can be seen in the top-left panel of Figure 2 where $||p_t - \hat{p}_t(t)|| \approx 27$ m. On the other hand, as the mission unfolds and several re-planning events occur, more accurate estimates are passed to the planner, which ultimately steers the formation toward the transmitter. This can be seen in the bottom-right panel of Figure 2.

As it was previously mentioned, maximum velocity and minimum inter-vehicle safety distance constraints are imposed. The right side of Figure 3 shows the speed profile of the vehicles. It can be seen that when the trajectory re-planning takes place, the speeds of the vehicles match the current speed at

Authorized licensed use limited to: Universita degli Studi di Roma La Sapienza. Downloaded on July 13,2023 at 11:03:11 UTC from IEEE Xplore. Restrictions apply.

which they were previously moving, therefore satisfying the initial velocity constraint. Furthermore, the velocity obtained satisfies the feasibility constraint, i.e., $||\dot{p}_{N,k}(t)|| \leq v_{k,max} = 5$ m/s. Finally, the right side of Figure 3 shows that the safety distance among the vehicles is kept for all times, i.e., $||p_{N,k}(t) - p_{N,j}(t)|| \geq d_{safe} = 3$ m $\forall t \geq 0$. It is worth noting that the problem formulation can be seamlessly extended by including additional constraints. For example, an additional boundary condition can be imposed on the acceleration, i.e., $\ddot{p}_{d,k}(t_0) = \ddot{p}_{k,t_0}$, to ensure that the overall acceleration profile is continuous.

Lastly, we note that using multiple vehicles as opposed to a single agent, it is possible to obtain relatively simple trajectories which are sufficiently excited to guarantee an accurate estimation of the transmitter location.

VI. Conclusion

In this work, we presented an optimal motion planning algorithm for search and rescue missions. The method generates trajectories for multiple agents that satisfy feasibility and safety constraints, while minimizing the actuation effort and maximizing a function describing the victims' observability. The computational efficiency of the algorithm enables real-time implementation and fast re-planning. These properties are exploited to achieve robustness and efficient execution of the victim localization mission. Future work includes the formulation of event-triggered re-planning strategies with provable stability of the estimation/motion planning closed-loop architecture.

References

[1] C. Sampedro, A. Rodriguez-Ramos, H. Bavle, A. Carrio, P. de la Puente, and P. Campoy, "A fully-autonomous aerial robot for search and rescue applications in indoor environments using learning-based techniques," *J. Intell. Robot. Syst.*, vol. 95, no. 2, pp. 601–627, 2019.

[2] S. Waharte and N. Trigoni, "Supporting search and rescue operations with UAVs," in *Proc. Int. Conf. Emerg. Security Technol.*, 2010, pp. 142–147.

[3] T. Tomic *et al.*, "Toward a fully autonomous UAV: Research platform for indoor and outdoor urban search and rescue," *IEEE Robot. Autom. Mag.*, vol. 19, no. 3, pp. 46–56, Sep. 2012.

[4] M. A. Goodrich *et al.*, "Supporting wilderness search and rescue using a camera-equipped mini UAV," *J. Field Robot.*, vol. 25, nos. 1–2, pp. 89–110, 2008.

[5] L. Marconi *et al.*, "The SHERPA project: Smart collaboration between humans and ground-aerial robots for improving rescuing activities in alpine environments," in *Proc. IEEE Int. Symp. Safety Security Rescue Robot. (SSRR)*, 2012, pp. 1–4.

[6] *Aerial Robotic Technologies for Professional Search and Rescue*. Accessed: Nov. 23, 2020. [Online]. Available: https://www.airborne-project.eu/

[7] N. Mimmo, P. Bernard, and L. Marconi, "Avalanche victim search via robust observers," *IEEE Trans. Control Syst. Technol.*, early access, Sep. 14, 2020, doi: 10.1109/TCST.2020.3016665.

[8] G. Indiveri, P. Pedone, and M. Cuccovillo, "Fixed target 3D localization based on range data only: A recursive least squares approach," *IFAC Proc. Vol.*, vol. 45, no. 5, pp. 140–145, 2012.

[9] P. Salaris, M. Cognetti, R. Spica, and P. R. Giordano, "Online optimal perception-aware trajectory generation," *IEEE Trans. Robot.*, vol. 35, no. 6, pp. 1307–1322, Dec. 2019.

[10] K. Dogancay, "UAV path planning for passive emitter localization," *IEEE Trans. Aerosp. Electron. Syst.*, vol. 48, no. 2, pp. 1150–1166, Apr. 2012.

[11] S. Minaeian, J. Liu, and Y.-J. Son, "Vision-based target detection and localization via a team of cooperative UAV and UGVs," *IEEE Trans. Syst., Man, Cybern., Syst.*, vol. 46, no. 7, pp. 1005–1016, Jul. 2016.

[12] N. T. Hung, N. Crasta, D. Moreno-Salinas, A. M. Pascoal, and T. A. Johansen, "Range-based target localization and pursuit with autonomous vehicles: An approach using posterior CRLB and model predictive control," *Robot. Auton. Syst.*, vol. 132, Oct. 2020, Art. no. 103608.

[13] A. V. Rao, "A survey of numerical methods for optimal control," *Adv. Astronaut. Sci.*, vol. 135, no. 1, pp. 497–528, 2009.

[14] J. T. Betts, *Practical Methods for Optimal Control and Estimation Using Nonlinear Programming*. Philadelphia, PA, USA: SIAM, 2010.

[15] J. T. Betts, "Survey of numerical methods for trajectory optimization," *J. Guid. Control Dyn.*, vol. 21, no. 2, pp. 193–207, 1998.

[16] B. A. Conway, "A survey of methods available for the numerical optimization of continuous dynamic systems," *J. Optim. Theory Appl.*, vol. 152, no. 2, pp. 271–306, 2012.

[17] P. Elijah, *Optimization: Algorithms and Consistent Approximations*. New York, NY, USA: Springer, 1997.

[18] A. Schwartz and E. Polak, "Consistent approximations for optimal control problems based on Runge–Kutta integration," *SIAM J. Control Optim.*, vol. 34, no. 4, pp. 1235–1269, 1996.

[19] A. L. Schwartz, "Theory and implementation of numerical methods based on Runge–Kutta integration for solving optimal control problems," Ph.D. dissertation, Dept. Electr. Eng. Comput. Sci., Univ. California, Berkeley, CA, USA, 1996.

[20] I. M. Ross and M. Karpenko, "A review of pseudospectral optimal control: From theory to flight," *Annu. Rev. Control*, vol. 36, no. 2, pp. 182–197, 2012.

[21] V. Cichella, I. Kaminer, C. Walton, N. Hovakimyan, and A. Pascoal, "Bernstein approximation of optimal control problems," 2018. [Online]. Available: arXiv:1812.06132.

[22] V. Cichella, I. Kaminer, C. Walton, N. Hovakimyan, and A. M. Pascoal, "Consistent approximation of optimal control problems using bernstein polynomials," in *Proc. IEEE 58th Conf. Decis. Control (CDC)*, 2019, pp. 4292–4297.

[23] V. Cichella, I. Kaminer, C. Walton, and N. Hovakimyan, "Optimal motion planning for differentially flat systems using bernstein approximation," *IEEE Control Syst. Lett.*, vol. 2, no. 1, pp. 181–186, Jan. 2018.

[24] V. Cichella, I. Kaminer, C. Walton, N. Hovakimyan, and A. M. Pascoal, "Optimal multi-vehicle motion planning using Bernstein approximants," *IEEE Trans. Autom. Control*, early access, Jun. 1, 2020, doi: 10.1109/TAC.2020.2999329.

[25] C. Kielas-Jensen and V. Cichella, "BeBOT: Bernstein polynomial toolkit for trajectory generation," in *Proc. IEEE/RSJ Int. Conf. Intell. Robots Syst. (IROS)*, 2019, pp. 3288–3293.

[26] R. T. Farouki, "The Bernstein polynomial basis: A centennial retrospective," *Comput. Aided Geom. Design*, vol. 29, no. 6, pp. 379–419, Aug. 2012.

[27] J. Cacace, A. Finzi, V. Lippiello, M. Furci, N. Mimmo, and L. Marconi, "A control architecture for multiple drones operated via multimodal interaction in search & rescue mission," in *Proc. IEEE Int. Symp. Safety Security Rescue Robot. (SSRR)*, 2016, pp. 233–239.

[28] P. A. Ioannou and J. Sun, *Robust Adaptive Control*. Chelmsford, MA, USA: Courier Corp., 2012.

[29] R. E. Kalman, "A new approach to linear filtering and prediction problems," *J. Basic Eng.*, vol. 82, no. 1, pp. 35–45, 1960.

[30] S. Van Huffel and P. Lemmerling, *Total Least Squares and Errors-in-Variables Modeling: Analysis, Algorithms and Applications*. Dordrecht, The Netherlands: Springer, 2013.

[31] V. Cichella *et al.*, "A 3D path-following approach for a multirotor UAV on SO(3)," *IFAC Proc. Vol.*, vol. 46, no. 30, pp. 13–18, 2013.

[32] I. Kaminer, A. M. Pascoal, E. Xargay, N. Hovakimyan, V. Cichella, and V. Dobrokhodov, *Time-Critical Cooperative Control of Autonomous Air Vehicles*, Butterworth-Heinemann, Oxford, U.K., 2017.

[33] R. Naldi, M. Furci, R. G. Sanfelice, and L. Marconi, "Robust global trajectory tracking for underactuated VTOL aerial vehicles using inner-outer loop control paradigms," *IEEE Trans. Autom. Control*, vol. 62, no. 1, pp. 97–112, Jan. 2017.

[34] W. Xie, G. Yu, D. Cabecinhas, R. Cunha, and C. Silvestre, "Global saturated tracking control of a quadcopter with experimental validation," *IEEE Control Syst. Lett.*, vol. 5, no. 1, pp. 169–174, Jan. 2021.

[35] C. Kielas-Jensen and V. Cichella, "Bernstein polynomial-based transcription method for solving optimal trajectory generation problems," 2020. [Online]. Available: arXiv:2010.09992.

[36] *Bernstein/Bézier Trajectory Toolkit*. Accessed: Jul. 31, 2019. [Online]. Available: https://github.com/caslabuiowa/OptimalBezierTrajectoryGeneration.

Authorized licensed use limited to: Universita degli Studi di Roma La Sapienza. Downloaded on July 13,2023 at 11:03:11 UTC from IEEE Xplore. Restrictions apply.